Molecular Crystals and Liquid Crystals

Publication details, including instructions for authors and subscription information:
http://www.tandfonline.com/loi/gmcl20

Temperature Dependence of Dielectric Behaviour of Mhpb(H)Pbc Antiferroelectric Liquid Crystal

M. Pandey [a] , R. Dhar [a] , V. Agrawal [b] & R. Dabrowski [c]

[a] Physics Department, Ewing Christian College, Allahabad, 211 003, India

[b] Physics Department, Allahabad University, Allahabad, 211 002, India

[c] Institute of Chemistry, Military University of Technology, Warsaw, 00-908, Poland

Version of record first published: 18 Oct 2010

To cite this article: M. Pandey, R. Dhar, V. Agrawal & R. Dabrowski (2004): Temperature Dependence of Dielectric Behaviour of Mhpb(H)Pbc Antiferroelectric Liquid Crystal, Molecular Crystals and Liquid Crystals, 414:1, 63-76

To link to this article: http://dx.doi.org/10.1080/15421400490427548

Mol. Cryst. Liq. Cryst., Vol. 414, pp. 63–76, 2004

ISSN: 1542-1406 print/1563-5287 online
DOI: 10.1080/15421400490427548

TEMPERATURE DEPENDENCE OF DIELECTRIC BEHAVIOUR OF MHPB(H)PBC ANTIFERROELECTRIC LIQUID CRYSTAL

M. B. Pandey and R. Dhar
Physics Department, Ewing Christian College, Allahabad-211 003, India

V. K. Agrawal
Physics Department, Allahabad University, Allahabad-211 002, India

R. Dabrowski
Institute of Chemistry, Military University of Technology, 00-908, Warsaw, Poland

Temperature dependence of dielectric behavior of antiferroelectric liquid crystal, MHPB(H)PBC, has been investigated in the frequency range of 1 Hz to 10 MHz. The experimental results have been analyzed using a generalized Cole–Cole expression. There is mainly one relaxation mechanism in SmA phase, which behaves as soft mode. Two dielectric relaxation processes have been observed in SmC_A^* phase, one at about 50 kHz and the other at about 400 kHz. Dielectric strengths of both modes remain constant throughout the SmC_A^* phase, while relaxation frequencies of both modes decrease with decrease in temperature. These two observed modes have been assigned to the in-phase and antiphase azimuthal fluctuations of the director of molecules in the antitilt pairs.*

Keywords: antiferroelectricity; dielectric relaxation; ionic conductivity; soft mode

INTRODUCTION

Since the discovery of chiral antiferroelectric smectic C_A^* (SmC_A^*) phase in MHPOBC by Chandani et al. [1], considerable attention has been paid

We thank University Grants Commission (UGC), New Delhi for financial assistance under major research project No. 10-81/2001. M. B. Pandey thanks UGC especially for a research fellowship under the project.

Address correspondence to R. Dhar, e-mail: dr_ravindra_dhar@rediffmail.com

to antiferroelectric liquid crystal (AFLC) from the viewpoint of not only fundamental structure and properties but also from their application to electro-optical devices. In the SmC_A^* phase, the molecules are oriented similar to those of ordinary ferroelectric liquid crystals (FLCs) in each smectic layer, but the orientation correlation of molecules in different layers is supposed to be quite different in two cases. The molecules in neighboring layers are tilted in opposite direction with respect to the layer normal in the antiferroelectric states; thus the net dipole moments of two adjacent layers are cancelled out, which implies the lack of macroscopic spontaneous polarization. Materials exhibiting antiferroelectric phases possess mostly the phase sequence I-SmA*-SmC_α^*-SmC*-SmC_γ^*-SmC_A^*, where I, SmA*, SmC_α^*, SmC*, SmC_γ^*, and SmC_A^* are the isotropic, paraelectric, incommensurate, ferroelectric, ferrielectric, and antiferroelectric phases, respectively [1]. This phase sequence is found in the materials with extremely high optical purity. In some AFLC materials, direct paraelectric-to-antiferroelectric transition has also been found [2–4]. The latter phase sequence is very attractive from the viewpoint of dielectric study, since there is no spontaneous polarization; the soft mode behavior is expected to be easily observed around the SmC_A^*-SmA* phase transition without applying any bias field.

The dielectric study of a large number of antiferroelectic liquid crystals has been reported, and possible information about the molecular orientation and the relaxation processes have been discussed [1–11]. However, the molecular aspect of the relaxation processes in SmC_A^* phase is still a matter of debate. In order to recognize and describe the structural features and phase transition behavior, it is necessary to accumulate more information about the structural parameters, which may then be referred to as basic data for determining some models of free energy potentials. For this purpose a new compound (5)-(+)-4-(1-methylheptyloxycarbonyl)phenyl-4′-(3-butanoiloxyprop-1-oxy)biphenyl-4′-carboxylate (in short, MHPB(H)-PBC) was synthesized, which exhibits only paraelectric (SmA*) and antiferroelectric (SmC_A^*) phases [12]. The electro-optic study of this compound was reported earlier [2]. In this work, we are reporting temperature dependence of the dielectric properties. By means of fitting operation, it has been possible to evaluate the characteristic parameters of each relaxation process. The structural changes in two smectic phases and in the vicinity of phase transitions was also analyzed on the basis of dielectric behavior.

EXPERIMENTAL

The liquid crystalline mesophases were identified with the help of transmitting light polarizing microscope equipped with hot stage and thermal

control unit. Mesophase transition temperatures were determined by using a differential scanning calorimeter (DSC) of Perkin Elmer equipped with TAC-7/DX controller and Pyris Software. Dielectric studies from 1 Hz to 10 MHz were carried out on planar aligned sample. The sample cell was prepared by using indium tin oxide (ITO)-coated glass plates having sheet resistance $\sim 25\,\Omega$. The planar alignment of the molecules has been achieved by depositing a thin layer of polyamide nylon on ITO-coated glass electrodes and then rubbing the electrodes unidirectionally with soft cotton. Two plates of the cell have been separated by mylar spacers of thickness 10 μm. Active capacitance (C_L) of the cell has been determined by filing standard organic liquid of known permittivity. The cell has been first filled with the samples in the isotropic phase by capillary action and then cooled slowly to get planar alignment. Dielectric data have been acquired using Impedance/Gain-Phase Analyzer of Solartron model SI-1260 coupled with Solartron dielectric interface model – 1296. Data lying between 100 Hz to 10 MHz were reverified using a Hewlett Packard Impedance/Gain-Phase Analyzer HP-4194A. While taking the dielectric observation, the sample was cooled at the scanning rate of 0.05 °C/min. Measured data above 1 MHz are affected due to finite resistance of ITO coated on glass plates and leads' inductance [13]. A measuring electric field of 0.5 Vrms was applied across the sample in the direction parallel to the smectic layers.

Instrumental uncertainty in the determination of transition temperature with the help of DSC is ± 0.1 °C. Temperatures of the sample for optical texture and dielectric studies have been controlled with the help of a hot stage of Instec (model HS-1) with the temperature accuracy of ± 3 mK. Temperature near the sample has been determined by measuring thermo emf of a copper-constantan thermocouple with the help of six and half digit multimeter. The uncertainty of the measurement of dielectric permittivity ($\varepsilon'_\perp$) and dielectric loss ($\varepsilon''_\perp$) within the entire frequency range is less than $\pm 2\%$. Other details of experimental techniques have already been discussed elsewhere [14,15].

The complex dielectric permittivity $\varepsilon^*(\omega, T)$ for the symmetric distribution of Cole–Cole type [16] is given by

$$\varepsilon^*(\omega, \mathrm{T}) = \varepsilon'(\infty) + \sum_{\mathrm{i}} \frac{(\Delta\varepsilon)_{\mathrm{i}}}{1 + (\mathrm{j}\omega\tau_{\mathrm{i}})^{1-\mathrm{h_i}}}, \tag{1}$$

where $\Delta\varepsilon_{\mathrm{i}}, \tau_{\mathrm{i}}$, and $\mathrm{h_i}$ are the dielectric strength, relaxation time, and symmetric distribution parameter ($0 \leq \mathrm{h_i} \leq 1$), respectively, of the ith mode, and $\varepsilon'(\infty)$ is the high frequency limiting value of dielectric permittivity. The dielectric strength ($\Delta\varepsilon$) of each mode is defined as the difference between the dielectric permittivity measured at low and high frequencies

of a relaxation region. Real and imaginary part of Equation (1) can be written as

$$\varepsilon' = \varepsilon'(\infty) + \sum_{i} \frac{\Delta\varepsilon_i[1 + (\omega\tau_i)^{(1-h_i)} \sin(h_i\pi/2)]}{1 + (\omega\tau_i)^{2(1-h_i)} + 2(\omega\tau_i)^{(1-h_i)} \sin(h_i\pi/2)} \tag{2}$$

and

$$\varepsilon'' = \sum_{i} \frac{\Delta\varepsilon_i(\omega\tau_i)^{(1-h_i)} \cos(h_i\pi/2)}{1 + (\omega\tau_i)^{2(1-h_i)} + 2(\omega\tau_i)^{(1-h_i)} \sin(h_i\pi/2)} \tag{3}$$

In the presence of electrode polarization capacitance and ionic conductance [17], $\varepsilon'(\mathrm{dc})f^{(-n)}$ and $\sigma(\mathrm{dc})/\varepsilon_0\omega$ terms are added in Equations (2) and (3), respectively. $\sigma(\mathrm{dc})$ is the ionic conductance and ε_0 ($=8.85$ pF/m) is the free-space permittivity. The measured dielectric absorption ε'' contains a spurious contribution in the high-frequency region of the spectrum due to finite resistance of ITO-coated electrodes [13]. An additional term Af^m is added in Equation (3) to partially account for ITO effect, where A and m are constants. The factor A depends on the reactive cutoff frequency of the cell, originating from resistance of the ITO layer, inductance of the leads, and capacitance of the cell. For thinner cells the cutoff frequency will be lower than the thicker cell [13]. Thus in order to resolve high-frequency absorption in the dielectric spectrum, it is preferable to use a thicker cell. The experimental data of frequency dependence of real part ($\varepsilon'_\perp$) and imaginary part ($\varepsilon''_\perp$) of complex dielectric permittivity were analyzed by fitting Equations (2) and (3) with the help of computer program (Origin Software). The computer program finds the mean deviation of the dielectric permittivity (calculated from the fitted parameter) from the measured values, minimizes it, and finds the optimum parameters, and also displays the fitted curve relative to the experimental curve. The input to the program is the first approximations to these parameters, these are guessed in the first instance from the experimental curve. An example of mode analysis at 63.0 °C is shown in Figure 1. Accuracy of estimation of these parameters is well within $\pm 10\%$ as reported earlier [8].

RESULTS AND DISCUSSION

Transition temperatures and hence phase sequence were determined with the help of DSC and Polarizing Microscope. DSC observations are taken at various scanning rates (SR) between 1.0 and 10.0 °C/min in the heating and cooling cycles. The DSC thermogram in the cooling cycle at the scanning rate of -1.0 °C/min is shown in Figure 2. Finite difference between the

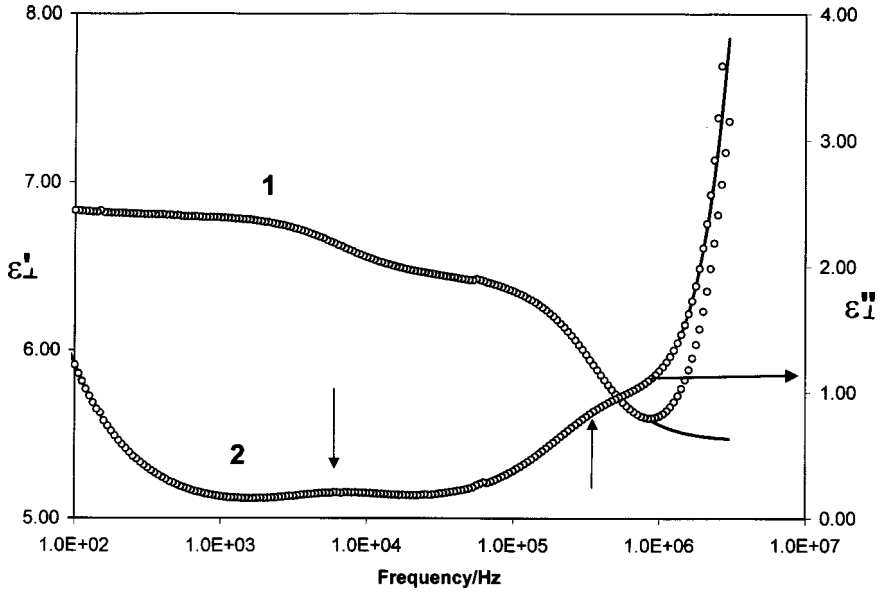

FIGURE 1 An example of mode separation by simulation of experimental data using Equations (2) and (3). Curve 1 shows frequency dependence of dielectric permittivity ($\varepsilon'_{\perp}$) and curve 2 shows frequency dependence of dielectric loss ($\varepsilon''_{\perp}$) in the antiferroelectric phase SmC_A^* at 63.0°C. The open circles represent experimental data, and the solid lines represent fitted curve. Data lying between 1 Hz and 100 Hz have not been shown here to enhance the visualization of two modes of dielectric relaxation (marked by vertical arrows), which are otherwise masked due to the electrode polarization/ionic effects present below 100 Hz.

transition temperatures (T_p) recorded during the heating and cooling cycles was observed even for the enantiotropic transitions, and it increases with SR. It was observed that T_p depends linearly with SR with positive and negative slopes in heating and cooling cycles, respectively [18]. Extrapolation of T_p versus SR plots to the scanning rate of 0 °C/min give true transition temperature (under the condition of virtual thermal equilibrium), which happens to be same during heating and cooling cycles for an enantiotropic transition [18]. Thus phase sequence K—66.4 °C (SmI* 38.2°C←) → SmC_A^* ←(90.3 °C) → SmA* ← (115.5 °C) → I was determined, where K represents crystal phase. SmC_A^* phase shows super cooling effect as reported in other material also [11] and goes to SmI* phase at 38.2°C in the cooling cycle.

The temperature dependence of the real part of dielectric permittivity ($\varepsilon'_{\perp}$) at different frequencies is shown in Figure 3, which clearly reveals the existence of two phases in the sample, i.e., SmA* and SmC_A^*. SmA*

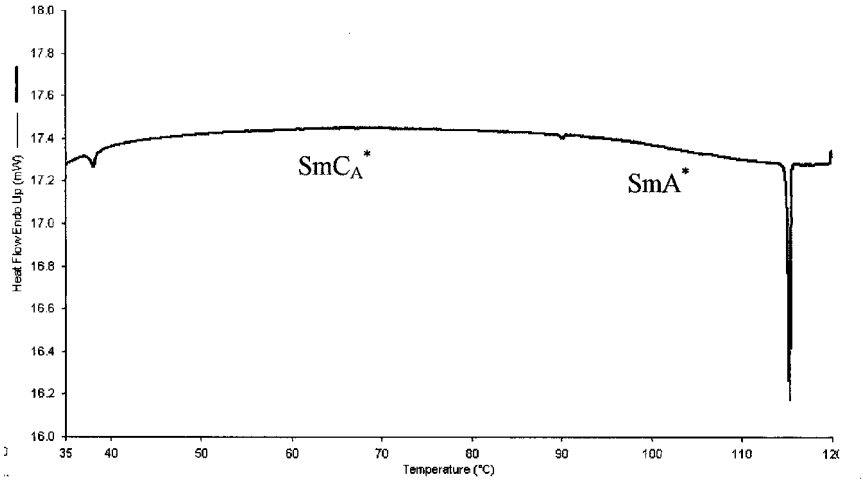

FIGURE 2 DSC thermogram in the cooling cycle at the scanning rate of $1.0^{\circ}\mathrm{C\,min^{-1}}$.

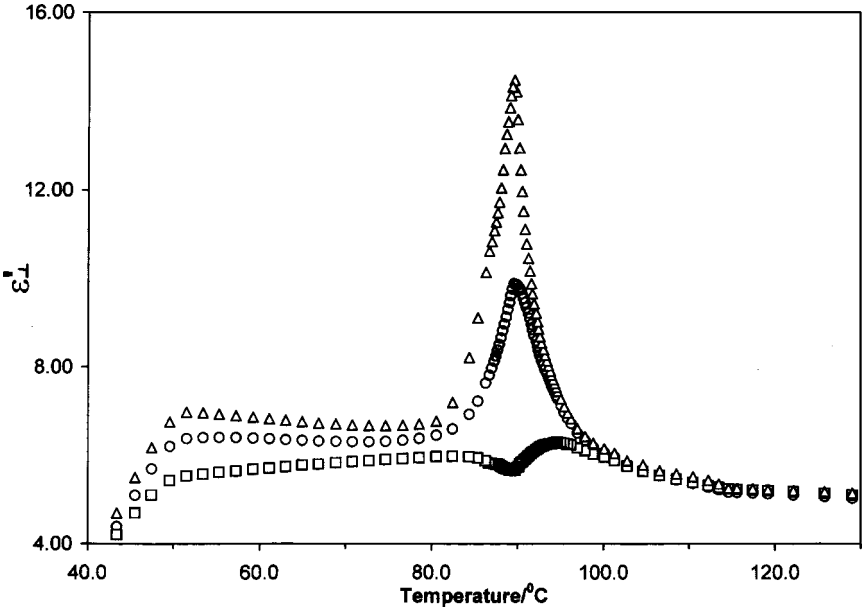

FIGURE 3 Temperature dependence of real part of dielectric permittivity ($\varepsilon'_{\perp}$) for three different frequencies, 1 kHz, 100 kHz, and 500 kHz, represented by open triangles, circles, and squares, respectively.

and SmC_A^* transition is clearly visible by the peak of $\varepsilon'_\perp$ observed at $89.5 \pm 0.2\,^\circ C$. The continuous change of $(\varepsilon'_\perp)$ at SmA^*–SmC_A^* transition temperature ($T_{A^*C_A^*}$) indicates weakly first-order nature of the SmA^*–SmC_A^* transition. The Cole–Cole diagram for SmA^* and SmC_A^* phases at $92.7\,^\circ C$ and $61.1\,^\circ C$, respectively, are shown in Figure 4. From Figure 4 it is evident that only one relaxation, i.e., soft mode is present in the SmA^* phase, whereas two relaxation modes are present in SmC_A^* phase. Figures 5 and 6 show the temperature dependence of dielectric strength ($\Delta\varepsilon$) and relaxation frequency (f_R) obtained from fitting the dielectric spectra. In SmA^* phase, increase of the dielectric strength observed near $T_{A^*C_A^*}$ is due to the contribution of soft mode as observed by other workers as well [3–10]. The soft mode contribution in SmA^* phase above $100\,^\circ C$ could not be detected due to weak dielectric strength and dominating high frequency effect above 1 MHz. In SmA^* phase, the relaxation frequency shows the expected slowing down behaviour with decreasing temperature. Relaxation frequency has no discontinuity at the transition temperature ($T_{A^*C_A^*}$).

The dielectric spectrum of the SmC_A^* phase (see Figure 1) contains two absorption peaks P_L (lower frequency mode) and P_H (higher frequency mode) separated by at least a decade of frequency at all temperatures. The dielectric strength of P_L and P_H mode are less than one order of magnitude in comparison to dielectric strength of soft mode of SmA^* phase. The temperature dependence of dielectric strengths and relaxation frequencies of P_L and P_H modes are shown in Figures 5 and 6, respectively. Although the dielectric strengths are small for both modes as obtained by Moritake et al. [3], clear relaxation peaks were observed in absorption spectrum of dielectric permittivity. The relaxation frequency (f_H) of P_H mode in SmC_A^* phase increases rapidly in the vicinity of $T_{A^*C_A^*}$ (from temperature $89.3\,^\circ C$ to $78.5\,^\circ C$) with decrease in temperature (see Figure 6). However, with decrease in temperature below $78.5\,^\circ C$, f_H decreases slowly and reaches to 100 kHz at lowest temperature of SmC_A^* phase, P_L mode of relaxation begins to appear in the vicinity of SmA^*–SmC_A^* transition, and its dielectric strength ($\Delta\varepsilon_L$) and relaxation frequency (f_L) decreases on cooling from $T_{A^*C_A^*}$. The P_L mode of relaxation was not resolved clearly near SmA^*–SmC_A^* transition, as reported by other workers [3,4], but appears as a shoulder with P_H mode because f_L is close to f_H, and the dielectric strength of P_H mode ($\Delta\varepsilon_H$) is larger than that of the P_L mode ($\Delta\varepsilon_L$).

On the basis of dielectric data discussed above it seems that SmC_A^* phase is stabilized only below $78\,^\circ C$. This is due to the competition between surface layer and bulk of the sample, because aligning surfactant forces the surface layer to stay in SmA^* phase well below $T_{A^*C_A^*}$ while bulk is in the SmC_A^* phase. In general it has been observed that the electrode surfaces tend to stabilize orthogonal SmA^*-like structure and destabilize antiferroelectric SmC_A^* phase [19]. It is important to note that clearly visible P_L

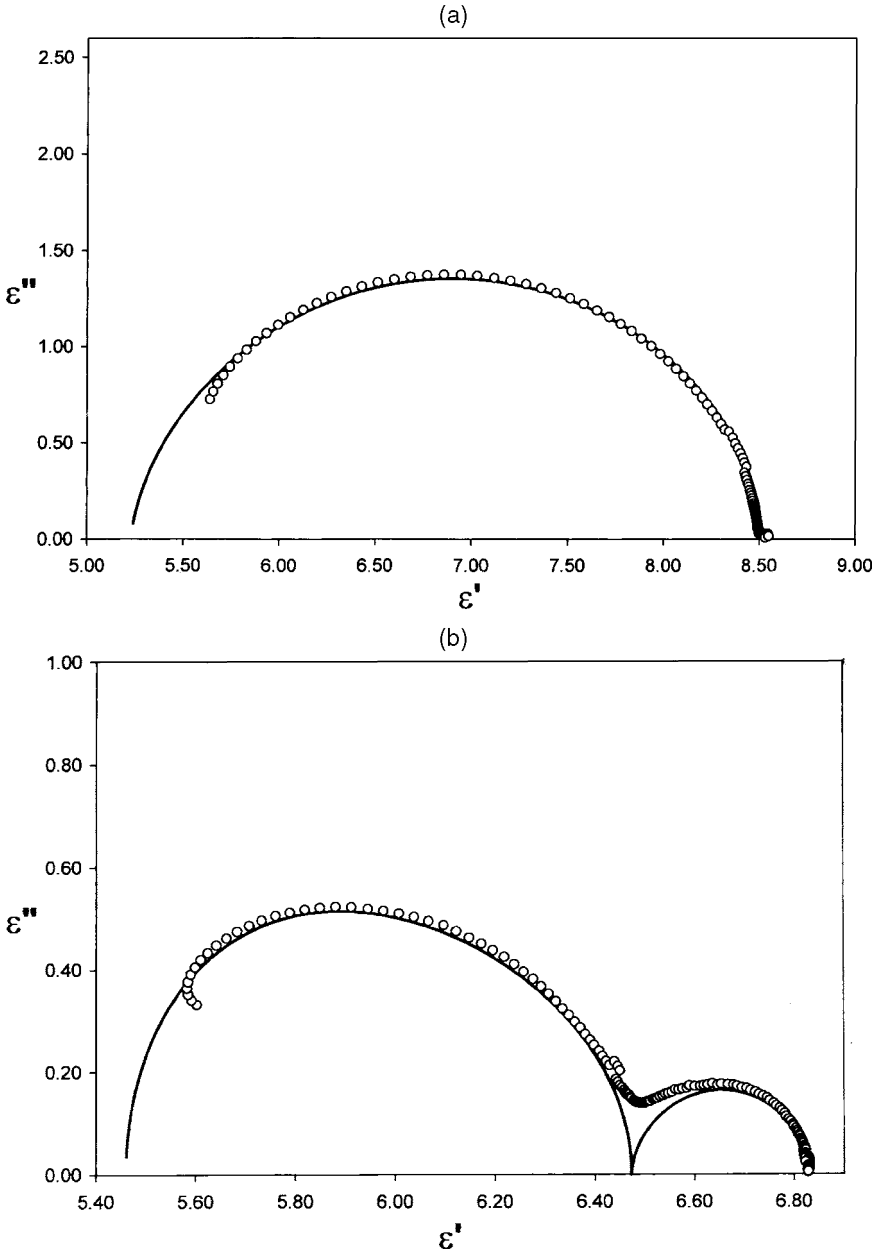

FIGURE 4 (a)Cole–Cole diagram in SmA* phase at 92.7°C. (b) Cole–Cole diagram in SmC_A^* phase at 61.1°C.

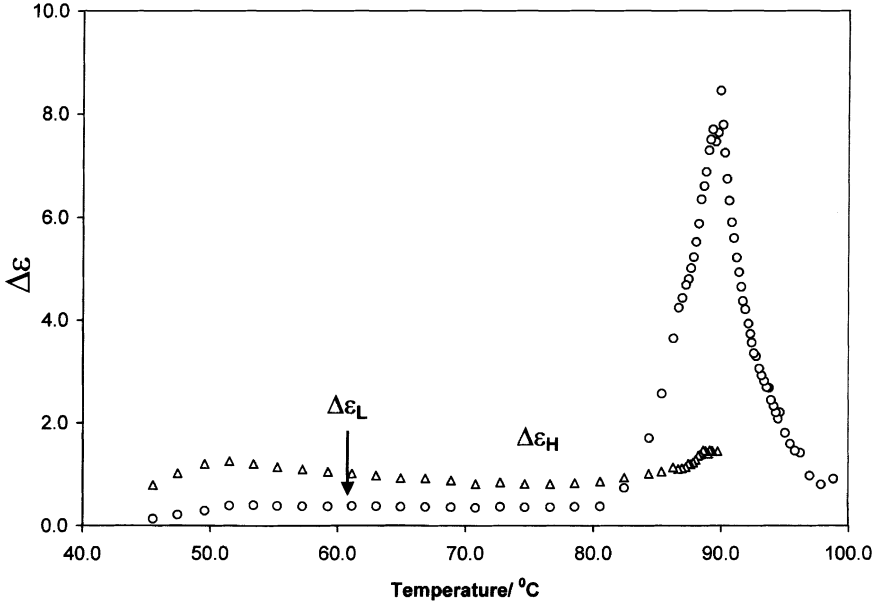

FIGURE 5 Temperature dependence of dielectric strengths ($\Delta\varepsilon$) of different modes in the SmA* and SmC_A^* phases.

mode has been observed only below 78 °C. However, we are able to detect P_L mode in the vicinity of SmA*–SmC_A^* transition by fitting Equations (2) and (3) on experimental data. f_L and $\Delta\varepsilon_L$ of P_L mode decrease with a decrease in temperature below SmA*–SmC_A^* transition temperature. Under the polarizing microscopic investigation also it has been observed that few focal conic fans reminiscent of SmA* phase continue to appear several degrees below SmA*–SmC_A^* transition temperature and disappear completely only below $\approx$78 °C. Below 80 °C, P_L mode shifts remarkably towards lower frequencies and its dielectric strength stabilizes. f_L is $\approx$1 kHz near the crystallization temperature.

Relaxation modes (P_L and P_H) discussed above appearing at different relaxation frequencies seem to be collective excitations [5]. The onset of antiferroelectric ordering at SmA*–SmC_A^* phase transition is characterized by a condensation of a nonpolar antiferroelectric soft mode that breaks the continuous symmetry of SmA* phase [20]. The condensation of soft mode has the effect of doubling of the smectic unit cell in SmC_A^* phase. Because of this doubling of the unit cell, the number of dispersion branches is doubled in the SmC_A^* phase. The doubling of a smectic unit cell at SmA*–SmC_A^* phase transition has implications for the spectrum of

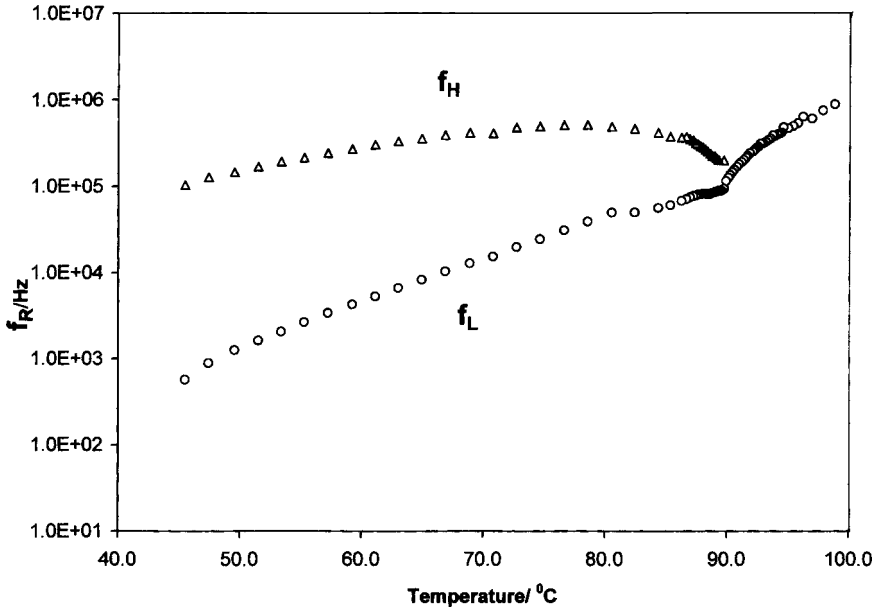

FIGURE 6 Temperature dependence of the relaxation frequencies (f_R) of different modes in the SmA* and SmC_A^* phases.

collective excitations of the SmC_A^* phase. These two modes are considered to be related to the antiphase and in-phase azimuthal angle fluctuation of the directors in the antitilted molecular pairs, respectively, as assigned by other workers [5].

At low frequencies another relaxation mode was observed below 10 Hz (see Figure 7) with d.c. tail. Such a relaxation mode at lower frequency was observed in some chiral mixtures, as reported by us [15] and by other workers in pure compounds also [10,21–22]. This mode was observed in all the phases, and its relaxation frequency remains constant at about 1.6 Hz in all the phases, but its dielectric strength decreases with decrease in temperature from the isotropic phase to antiferroelectric phase. This mode disappears near SmC_A^* to crystal transition. This mode also obeys generalized Cole–Cole Equation (1). Uehara et al. [10] observed two slow relaxation modes in antiferroelectric material MHFPDBC. One relaxation mode was reported at about 10^{-2} Hz, which happens to be present in all the mesophases, while another relaxation reported at about 1 Hz has been observed only in ferrielectric subphases. Uehara et al. [10] interpreted the low-frequency relaxation mode due to space charge accumulation between polyamide coating and liquid crystals, whereas high-frequency relaxation mode is due to rearrangement of complex ferrielectric layer

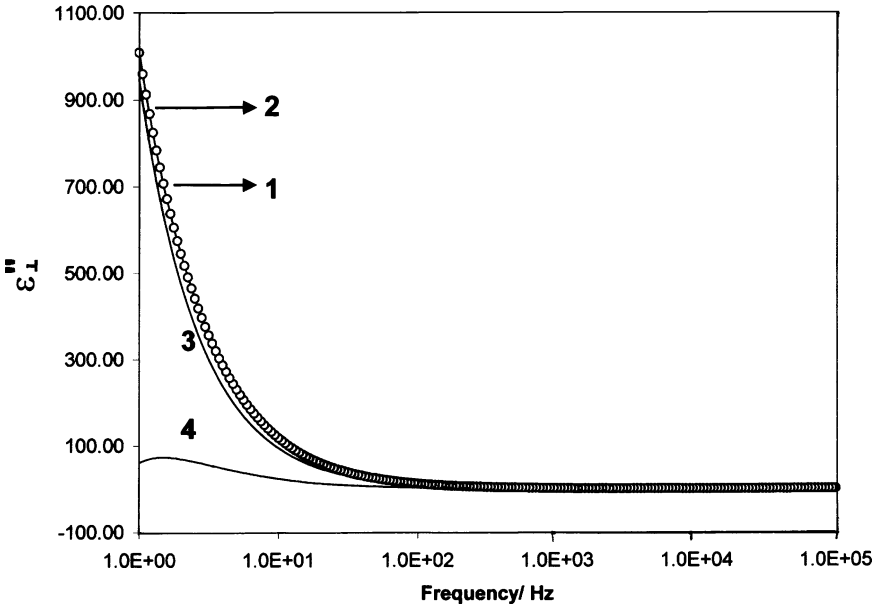

FIGURE 7 Variation of dielectric loss ($\varepsilon''_{\perp}$) showing ionic effect in low frequency region in SmA* phase (96.2°C): 1, $\varepsilon''_{\perp}$ (measured); 2, (fitted); 3, $\varepsilon''_{\perp}$(dc); 4, $\varepsilon''_{\perp}$ (measured)- $\varepsilon''_{\perp}$(dc).

structure with helix from unwound ferroelectric structure. Havrilliak et al. [21] have reported low-frequency relaxation mode in the SmC* phase of a FLC mixture at about 5 Hz, origin of which is other than the ionic impurities. In the case of our sample since the slow mode of relaxation exists in all the phases (except crystal), therefore it may be assigned to the ionic conductance. Space charge accumulation on the interface between liquid crystal and polyamide coating may be the origin of this mode, and there may not be any relation to structural motion.

σ(dc) has been determined in different mesophases by the fitting Equation (3) on dielectric spectra. It has been observed that σ(dc) decreases with decrease in temperature and it follows Arrhenius behavior:

$$\sigma(\mathrm{dc}) = \mathrm{A}_0 \exp\left(\frac{-\mathrm{W_a}}{\mathrm{kT}}\right), \tag{4}$$

where A_0 is a constant, $\mathrm{W_a}$ is the activation energy, T is the absolute temperature, and k ($=1.38 \times 10^{-23}$ J/K) is the Boltzman constant. Variation of ln(σ(dc)) with the inverse of absolute temperature (1/T) is shown in Figure 8. Activation energy for ionic conductance of different mesophases

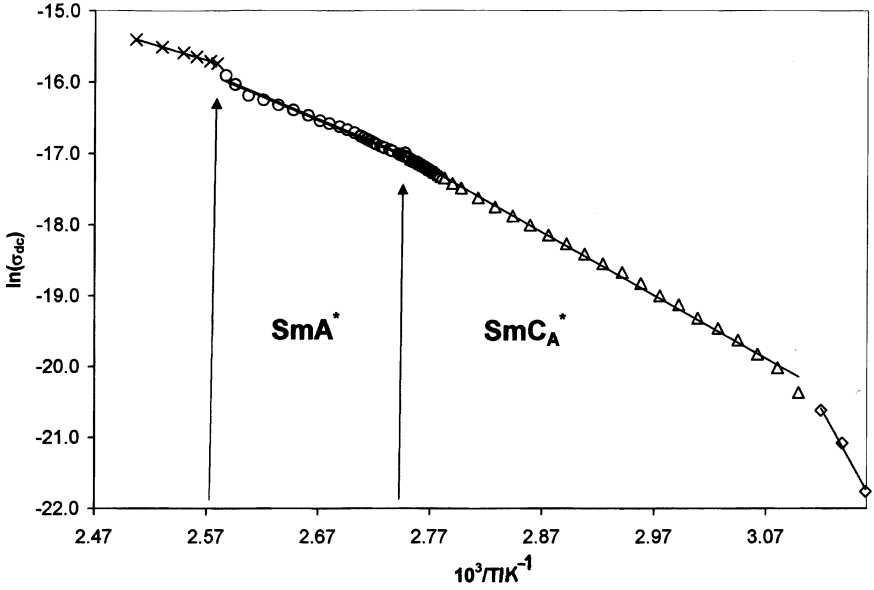

FIGURE 8 Variation of $\ln(\sigma(\mathrm{dc}))$ with inverse of absolute temperature $(10^3/\mathrm{T})$.

was determined with the help of least-square fit method. The value of activation energy in the isotropic phase is found to be 0.40 ± 0.01 eV, which has been reported by others as well [23]. In SmA* and $\mathrm{SmC_A}^*$ phases the value of the activation energies were found to be 0.54 ± 0.01 eV and 0.77 ± 0.01 eV, respectively. It is important to note that at the onset of SmA* phase, material transforms into the layered structure, and the movement of the ions parallel to the layers are restricted because the probability of collisions of ions with liquid crystal molecules increases and hence $\sigma(\mathrm{dc})$ decreases. As a result, increase in the activation energy has been observed. Similar results have been observed by us in some chiral liquid crystal mixtures [15].

An empirical formula has been proposed for the variation of ionic conductivity in a smectic structure as [24]

$$\sigma(\mathrm{z}) = \sigma_0 \left[1 + \mathrm{B}\sin\left(\frac{2\pi\,\mathrm{z}}{\mathrm{d}}\right)\right], \tag{5}$$

where d is the layer thickness and B is the function of the amplitude of the density. In $\mathrm{SmC_A}^*$ phase, layer thickness became nearly double in comparison to SmA* phase. Because the unit cell of homogenous antiferroelectric $\mathrm{SmC_A^*}$ phase consists of two smectic layers at opposite tilt to each other,

the ions will therefore be more restricted to move parallel to smectic layer and the probability of collisions of ions with liquid crystal molecules will be increased in comparison to SmA^* phase; therefore, decrease in $\sigma(dc)$ and increase in activation energy of SmC_A^* phase is expected.

CONCLUSION

In antiferroelectric liquid crystal, MHPB(H)PBC, one relaxation mode observed in SmA^* phase was identified as soft mode on the basis of its temperature dependence. Two other modes of relaxation observed in SmC_A^* phase were related to the antiphase and in-phase azimuthal angle fluctuation of molecules in antitilt pair. A slow mode of dielectric relaxation at about 1.6 Hz was observed in all phases, and it was assigned to ionic conductance.

REFERENCES

[1] (a) Chandani, A. D. L., Ouchi, Y., Takezoe, H., Fukuda, A., Terashima, K., Furukawa, K., & Kishi, A. (1989). Novel phases exhibiting tristable switching, *Jpn. J. Appl. Phys.*, *28*, L1261–1264.
(b) Chandani, A. D. L., Gorecka, E., Ouchi, Y., Takezoe, H., & Fukuda, A. (1989). Antiferroelectric chiral smectic phases responsible for the tristable switching in MHPOBC, *Jpn. J. Appl. Phys.*, *28*, L1265–1268.
[2] Raszewski, Z., Kedzierski, J., Rutkowska, J., Piecek, W., Perkowski, P., Czuprynski, K., Dabrowshki, R., Drzewinski, W., Zielinski, J., & Zmija, J. (2001). Determination of molecular parameters of the MHPB(H)PBC and MHPB(F)PBC antiferroelectric liquid crystals, *Mol. Cryst. Liq. Cryst.*, *366*, 607–616.
[3] Moritake, H., Ozaki, M., & Yoshino, K. (1993). DC-bias-field-induced dielectric relaxation in antiferroelectric phase of TFMHPOBC, *Jpn. J. Appl. Phys.*, *32*, L1432–1435.
[4] Hiraoka, K., Ouchi, Y., Takezoe, H., Fukada, A., Inui, S., Kawano, S., Saito, M., Iwane, H., & Itoh, K. (1991). Dielectric studies on antiferroelectric liquid crystals, *Mol. Cryst. Liq. Cryst.*, *199*, 197–205.
[5] Buivydas, M., Gouda, F., Lagerwall, S. T., & Stebler, B. (1995). The molecular aspect of double absorption peak in the dielectric spectrum of antiferroelectric liquid crystal phase. *Liq. Cryst.*, *18*, 879–886.
[6] Buivydas, M., Gouda, F., Andersson, G., Lagerwall, S. T., Stebler, B., Bomelburg, J., Heppke, G., & Gestblom, B. (1997). Collective and non-collective excitations in antiferroelectric and ferrielectric liquid crystals studied by dielectric relaxation spectroscopy and electro-optic measurement, *Liq. Cryst.*, *23*, 723–739.
[7] Hou, J., Schacht, J., Giebelmann, F., & Zugenmaier, P. (1997). Temperature and bias-field dependences of dielectric behaviour in the antiferroelectric liquid crystal, (R)-MHPOBC, *Liq. Cryst.*, *22*, 409–417.
[8] Panarin, Y. P., Kalinovskaya, O., & Vij, J. K. (1998). The investigation of relaxation processes in antiferroelectric liquid crystals by broad band dielectric and electro-optic spectroscopy, *Liq. Cryst.*, *25*, 241–252.
[9] Hatano, J., Hanakai, Y., Furue, H., Uehara, H., Satio, S., & Murashiro, K. (1994). Phase sequence in smectic liquid crystals having flurophenyl group in the core, *Jpn. J. Appl. Phys.*, *33*, 5498–5502.

[10] Uehara, H., Hanakai, Y., Hatano, J., Satio, S., & Murashiro, K. (1995). Dielectric relaxation modes in the phases of antiferroelectric liquid crystals, *Jpn. J. Appl. Phys.*, *34*, 5424–5428.
[11] O'Sullivan, J. W., Vij, J. K., and Nguyen, H. T. (1997). Polarization and dielectric properties of an antiferroelectric liquid crystal, *Liq. Cryst.*, *23*, 77–86.
[12] Drzewinski, W., Czuprynski, K., Dabrowski, R., Raszewski, Z., Rutkowska, J., Przedmojski, J., Gorecka, E., & Neubert, M. (1998). New analogous of MHPOBC, *SPIE Proc.*, *3319*, 100–104.
[13] Dhar, R. (2004). An impedance model to improve the higher frequency limit of electrical measurement on the capacitor cell made from electrodes of finite resistances, *Ind. J. Pure Appl. Phys.*, *42*, 56–61.
[14] Dhar, R., Pandey, M. B., & Agrawal, V. K. (2003). Twisted grain boundary phases in the binary mixture of 3β-chloro-5-cholestene and 4-n-decyloxybenzoic acids, *Phase Transitions*, *76*, 763–780.
[15] Pandey, M. B., Dhar, R., Agrawal, V. K., Khare, R. P., & Dabrowski, R. (2003). Low frequency dielectric spectroscopy of two room temperature chiral liquid crystal mixtures, *Phase Transitions*, *76*, 945–958.
[16] Hill, N. E., Vaughan, W. E., Price, A. H., & Davies, M. (1969). *Dielectric Properties and Molecular Behaviour* (London: Van Nostrand Reinhold Co.) pp. 1–106.
[17] Srivastava, S. L. & Dhar, R. (1991). Characteristic time of ionic conductance and electrode polarization capacitance in some organic liquids by low frequency dielectric spectroscopy, *Ind. J. Pure Appl. Phys.*, *29*, 745–751.
[18] Srivastava, S. L., Dhar, R., & Mukherjee, A. (1996). Thermodynamical properties of bicomponent mixtures of liquid crystals cholesteryl pelargonate and nonyloxybenzoic acid, *Mol. Cryst. Liq. Cryst.*, *287*, 139–154.
[19] Lagerwall, S. T. (1999). *Ferroelectric and Antiferroelectric Liquid Crystals* (Weinheim: Wiley-VCH) pp. 325–400.
[20] Musevic, I., Blinc, R., & Zeks, B. (2000). *The Physics of Ferroelectric and Antiferroelectric Liquid Crystals* (Singapore: World Scientific).
[21] Havrilliak, Jr., S., Vij, J. K., & Ni, M. (1999). Low frequency dielectric relaxation in the smectic C^* phase of a ferroelectric liquid crystal, *Liq. Cryst.*, *26*, 465–467.
[22] Kundu, S., Roy, S. K., Dabrowski, R., Ganzke, D., & Hasse, W. (2001). Electro-optic and dielectric properties of an antiferroelectric liquid crystal material, *Mol. Cryst. Liq. Cryst.*, *366*, 593–605.
[23] Jadzyn, J. & Czechowski, G. (1989). Dielectric study of nematic-smectic A-reentrant nematic transition in the 80CB/60CB mixtures, *Liq. Cryst.*, *4*, 157–163.
[24] Myrvold, B. O. & Coles, J. (1995). DC conductivity in smectic A phases-a breakdown of Kohlrausch's law, *Mol. Cryst. Liq. Cryst.*, *259*, 75–92.